Hot Electrons from Consecutive Exciton–Mn Energy Transfer in Mn-Doped Semiconductor Nanocrystals

ARTICLE *in* THE JOURNAL OF PHYSICAL CHEMISTRY C · MAY 2011

Impact Factor: 4.77 · DOI: 10.1021/jp2016598

6 AUTHORS, INCLUDING:

Hsiang-Yun Chen
University of California, Irvine
12 PUBLICATIONS **145** CITATIONS
SEE PROFILE

Tai-Yen Chen
Cornell University
19 PUBLICATIONS **96** CITATIONS
SEE PROFILE

THE JOURNAL OF PHYSICAL CHEMISTRY C

ARTICLE

pubs.acs.org/JPCC

Hot Electrons from Consecutive Exciton−Mn Energy Transfer in Mn-Doped Semiconductor Nanocrystals

Hsiang-Yun Chen,[†] Tai-Yen Chen,[†] Erick Berdugo,[†] Yerok Park,[†] Kaitlin Lovering,[‡] and Dong Hee Son*[,†]

[†]Department of Chemistry, Texas A&M University, College Station, Texas 77842, United States

[‡]Division of the Natural Science, New College of Florida, 5800 Bayshore Road, Sarasota, Florida 34243, United States

ABSTRACT: We investigated the generation of hot electrons occurring via two consecutive exciton−Mn energy transfer processes in Mn-doped semiconductor nanocrystals. Due to the fast exciton−Mn energy transfer rate combined with the long lifetime of the intermediate state of Mn^{2+} ions, consecutive energy transfer from two excitons to one Mn^{2+} ion can efficiently generate hot electrons even under weak cw excitation. The evidence for the occurrence of two consecutive energy transfers was obtained from the measurement of the intensity of luminescence from the excited state of Mn^{2+} ions serving as the intermediate acceptor state. Under the excitation condition, hot electrons can be generated via consecutive energy transfer, and Mn-doped nanocrystals also exhibit the stronger photoreducing capability of methylene blue than undoped nanocrystals, demonstrating a potential benefit in photocatalysis.

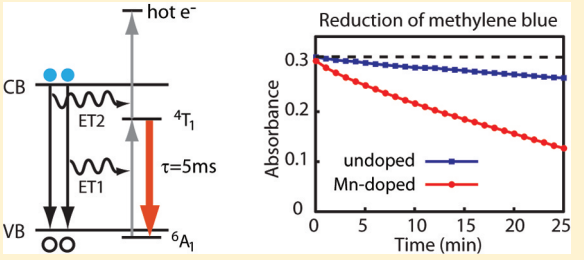

1. INTRODUCTION

Generation of hot electrons in metallic or semiconducting materials and hot electron-induced chemistry on their surfaces have been actively investigated for decades. For instance, optically excited hot electrons with excess energy above the Fermi level of metals demonstrated its capability to transfer part of the electron energy to the adsorbate molecules and excite their internal modes initiating various surface chemistries.[1−6] In semiconductors, hot electrons excited above the conduction band edge have been shown to be beneficial in catalysis and photovoltaic applications via fast interfacial charge transfer that can effectively compete with intraband relaxation.[7−9]

Recently, a number of groups reported efficient interfacial charge transfer of optically excited hot electrons in semiconductor nanocrystals,[10−12] demonstrating the potential of harvesting hot electrons in nanocrystals that are widely employed in catalysis and photovoltaic applications. Hot electrons with larger excess energy will generally experience a lower energy barrier for interfacial charge transfer, and their wave functions can reach further away from the nanocrystals, making them potentially useful for photocatalytic and photovoltaic applications.

Hot electrons in semiconductor nanocrystals can be excited via optical excitation in a number of different ways. The simplest way is the above-band-gap excitation with sufficient excess energy that can excite the electrons high in the conduction band. Hot electrons with higher excess energy generally require excitation with the higher-energy photons in the UV region, which is increasingly less convenient to work with. The lower-energy photons can also excite hot electrons with large excess energy via multiphoton excitation.[13−15] However, multiphoton excitation is usually much less efficient than single photon excitation and requires high excitation intensity.

In this study, we investigated the generation of hot electrons with large excess energy in Mn-doped semiconductor nanocrystals that occurs via two consecutive exciton−Mn energy transfer processes taking advantage of the fast exciton−Mn energy transfer and long lifetime of the intermediate acceptor state. In Mn-doped semiconductor nanocrystals such as Mn-doped CdS or ZnS, the energy of photoexcited excitons can be transferred to the excited ligand field state of Mn^{2+} ions. Typically, exciton−Mn energy transfer depletes the population of exciton and creates the locally excited ligand field state of Mn^{2+} ion ($^4T_1$) that has a lifetime of $\sim 10^{-3}$ s due to the dipole-forbidden nature of the transition involved.[16,17]

In principle, exciton−Mn energy transfer to the same Mn^{2+} ion can occur twice consecutively promoting Mn^{2+} ion to the higher-energy state if the second energy transfer occurs before the relaxation of the $^4T_1$ state of the Mn^{2+} ion. If such consecutive energy transfer occurs, the excited d-electron on Mn^{2+} ion at the terminal state is energetically located significantly above the conduction band edge of the semiconductor host. In this case, the excited state of Mn^{2+} ion after two consecutive energy transfers can be considered as Mn^{2+} ionized into the conduction band of the semiconductor host creating a delocalized hot electron and a hole localized near the Mn^{2+} ion.[18,19] Therefore, the overall effect of the two consecutive exciton−Mn energy transfers can be viewed as an "upconversion" of the energy of two excitons into one composed of a hot electron and a localized hole. Hot electron and localized hole pair created in this way ultimately

Received: February 19, 2011
Revised: April 20, 2011
Published: May 19, 2011

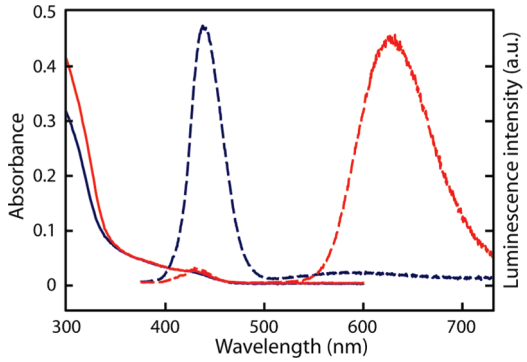

Figure 1. Absorption (solid) and luminescence (dashed) spectra of undoped (blue) and Mn-doped (red) CdS/ZnS nanocrystals. Excitation wavelength is 370 nm.

relax rather nonradiatively without significant recycling for the repopulation of the $^4T_1$ state.

Here, we present experimental evidence showing that two consecutive exciton−Mn energy transfers occur efficiently generating hot electrons in Mn-doped colloidal CdS/ZnS core/shell nanocrystals. The key evidence comes from the measurement of the luminescence intensity from the $^4T_1$ state of Mn^{2+} ion serving as the intermediate acceptor state at varying excitation densities under one- or two-pulse excitation conditions. We also show that Mn-doped nanocrystals exhibit a higher photocatalytic reducing capability of methylene blue than undoped nanocrystals when the excitation rate is sufficiently fast to have consecutive exciton−Mn energy transfer even under cw excitation conditions.

2. EXPERIMENTAL SECTION

Synthesis of Mn-Doped and Undoped CdS/ZnS Nanocrystals. Mn-doped and undoped CdS/ZnS core/shell nanocrystals of the same semiconductor host structures were synthesized for the comparative analysis of the photoluminescence intensity and photoreduction efficiency following the published methods and their variations.[20,21] Briefly, CdS core nanocrystals (3.6 nm in diameter) were synthesized by injecting the octadecene (ODE) solution of sulfur (0.25 M, 2.0 mL) to the mixture of cadmium oxide (0.126 g), oleic acid (2.02 g), and ODE (12.0 mL) heated at 250 °C. To coat ZnS shell on CdS core and Mn-doped CdS core, ODE solutions of sulfur and zinc stearate were added alternately to the ODE solution of CdS nanocrystals at 220 °C in the presence of oleylamine. In Mn-doped nanocrystals, Mn^{2+} ions were doped at the interface of CdS core and ZnS shell. Doping of Mn^{2+} ions was achieved by adding manganese diethyldithiolcarbamate dissolved in oleylamine to the solution of CdS core nanocrystals in ODE at 220 °C before putting ZnS shell. The average doping density of Mn^{2+} ions in Mn-doped nanocrystals was determined to be 3.6 ions per particle from the elemental analysis employing ICP mass spectrometry and the particle size measurement with TEM. Figure 1 shows the UV−vis absorption and luminescence spectra of both undoped and Mn-doped nanocrystals used in this study. Luminescence spectra of both nanocrystals were obtained with 370 nm excitation. The exciton and Mn luminescence in undoped and Mn-doped nanocrystals occur at 440 and 625 nm, respectively.

Excitation Density-Dependent Luminescence and Lifetime Measurement. The exciton and Mn luminescence intensities of undoped and Mn-doped nanocrystals were measured with 395 nm pulsed excitation within the fluence range of 0−4.6 mJ/cm^2 per pulse. The excitation pulses were generated by frequency doubling 790 nm output from a Ti:sapphire laser in a β-barium borate (BBO) crystal. The nanocrystal solution in hexane was circulated in a 1 mm thick liquid cell at the linear flow rate of ~1 cm/s to avoid any potential photodegradation of the nanocrystals by the excitation pulse. The repetition rate of the excitation pulse was set at 50 Hz, much slower than the relaxation time of the $^4T_1$ state on Mn^{2+} ions, to avoid the reexcitation of Mn-doped nanocrystal before the complete decay of Mn luminescence. The optical setup for the measurement of the luminescence intensity and lifetime is shown in Figure 2a. In order to obtain an accurate correlation between the luminescence intensity and excitation density of the nanocrystal (number of photons absorbed per particle), the spatial intensity profiles of both the excitation pulse and luminescence from the sample were measured. The spatially resolved detection of the luminescence intensity is particularly important when using excitation source with a small beam diameter. This is because Mn luminescence intensity becomes nonlinear to the excitation intensity as the excitation intensity increases, resulting in the mismatch of the spatial intensity profiles of excitation beam and Mn luminescence at higher excitation intensities.

The intensity profile of the excitation pulse was directly imaged with a CCD camera using a wedge beam splitter placed in front of the sample cell. The beam diameter (full width at half-maximum) measured in this way was ~500 μm. The intensity profile of the luminescence from the sample was measured by imaging the luminescence on the entrance of an optical fiber (50 μm in diameter) mounted on an $x-y$ translation stage. The exit side of the optical fiber was connected to a CCD spectrometer (QE65000, Ocean Optics) that measured both the spectrum and intensity of the luminescence as a function of the position of the optical fiber. The intensity profile of the luminescence was obtained by raster scanning the optical fiber. Figure 2b shows the spatial intensity profile of the excitation pulse at a low excitation fluence regime, where the luminescence intensity increases linearly with the excitation fluence. The line profiles of the excitation beam and Mn luminescence intensities are almost identical under this condition as shown on the top and right panels of Figure 2b. However, the two intensity profiles become more dissimilar as the excitation fluence increases. In this study, the excitation and luminescence intensities at the center of the peak within 50 μm diameter were taken to obtain excitation density-dependent luminescence intensity. For the lifetime measurement, the optical fiber was connected to a photomultiplier tube (931A, Hamamatsu), and the data were collected by a digital oscilloscope (TDS 2022B, Tektronix).

Photocatalysis Measurement. The kinetics of photocatalytic reduction of MB by undoped and Mn-doped nanocrystals was studied under 405 nm cw excitation. All the sample solutions were prepared in a N_2-atmosphere glovebox. Dichloromethane bubbled with N_2 for more than 1 h was used as the solvent to prevent oxidative photodegradation of MB by the dissolved oxygen. For the comparative measurement of the photoreduction rate by undoped and Mn-doped nanocrystals, concentrations of MB (6.1 μM) and nanocrystal (0.23 μM) and the total volume (2.1 mL) of the sample solution were kept identical for all the measurements. The sample solutions in the cuvette with an airtight cap were illuminated at two different excitation intensities, 760 and 1.2 mW/cm^2, using a diode laser and a light emitting diode, respectively. The absorbance of MB at 656 nm

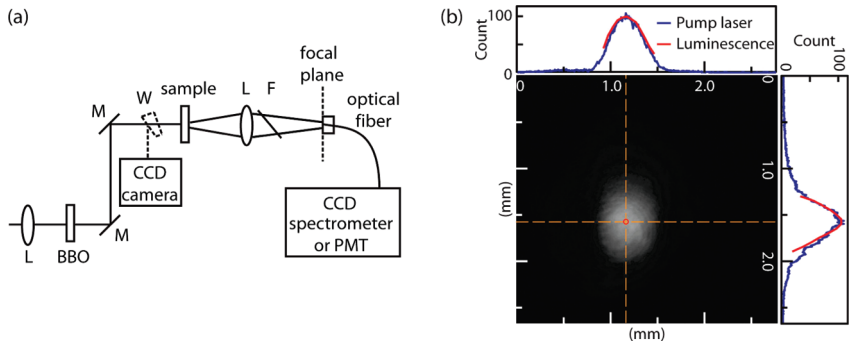

Figure 2. (a) Experimental setup for the measurement of excitation density-dependent luminescence intensity. L, M, W, and F are lens, dielectric mirror, wedge beam splitter, and filter, respectively. (b) Two-dimensional intensity profile of the excitation pulse at a low excitation fluence. The top and right panels compare the line profiles of the excitation (blue) and Mn luminescence intensities (red) in two directions indicated with the dashed line.

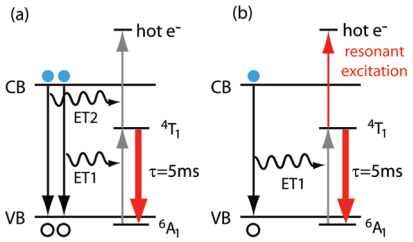

Figure 3. Possible pathways for hot electron excitation in Mn-doped CdS/ZnS nanocrystals. (a) Hot electron excitation via two consecutive exciton−Mn energy transfer processes in Mn-doped CdS/ZnS semiconductor nanocrystals. (b) Hot electron excitation via exciton−Mn energy transfer followed by a direct resonant excitation of the $^4T_1$ ligand field state of Mn^{2+} ion. VB and CB are valence and conduction band, respectively. Thick downward arrows in orange color indicate Mn luminescence. The lifetime of the $^4T_1$ state is 5 ms.

was recorded as a function of time to monitor the reduction kinetics. MB has negligible absorption at the excitation wavelength, and the illumination of the sample solution containing only MB showed virtually no change of absorbance during the period of time of the measurements.

3. RESULTS AND DISCUSSION

In Mn-doped CdS/ZnS nanocrystals, Mn luminescence arises from the radiative relaxation of $^4T_1$ ligand field state of Mn^{2+} ions populated by exciton−Mn energy transfer (ET1) to the ground $^6A_1$ state. If an additional exciton−Mn energy transfer (ET2) occurs to the same Mn^{2+} ion before the relaxation of the $^4T_1$ state, the $^4T_1$ state can be further excited to the conduction band level of the host leading to the ionization of Mn^{2+} to the conduction band as depicted in Figure 3a. Since the energy levels of Mn^{2+} d electrons are close to the valence band edge of CdS,[22,23] the two consecutive energy transfers (ET1 and ET2) to the same Mn^{2+} ion can create hot electrons with a large excess energy in the conduction band. The hole initially on Mn^{3+} will likely to be shared locally by the sulfur atoms nearby. Therefore, the resulting state from the two consecutive exciton−Mn energy transfers can be considered as a hot exciton composed of a hot electron and a localized hole near the Mn^{2+} ion. One might view this process as the "upconversion" of the energy of two excitons into a more energetic exciton via two energy transfer processes (eq 1) In this scheme, while the intermediate $^4T_1$ state is emissive the terminal state decays nonradiatively rather than decaying back to the $^4T_1$ state as will be discussed more in detail later.

$$Mn^{2+}(^6A_1) \xrightarrow{ET1} Mn^{2+}(^4T_1) \xrightarrow{ET2} Mn^{3+} + e_{CB} \quad (\text{or } Mn^{2+} + e_{CB} + h_{local}) \tag{1}$$

The confirmation of the occurrence of consecutive energy transfer from the spectroscopic detection of hot electrons is not straightforward in the steady state or time-resolved absorption measurements. This is because hot electrons in the conduction band do not have a sufficiently distinct spectroscopic signature from that of lower-energy electrons excited by the initial photoexcitation. However, the decrease of Mn luminescence from the depletion of the emitting $^4T_1$ state can be used as a readily measurable indicator of the occurrence of two consecutive energy transfers under the experimental condition that rules out other pathways to deplete the $^4T_1$ state. In fact, a decrease of Mn luminescence from the direct resonant excitation of the $^4T_1$ state to the conduction band following an exciton−Mn energy transfer has been observed in Mn-doped ZnSe nanocrystals by Irvine et al. under two-color cw excitation conditions as depicted in Figure 3b[18] (eq 2).

$$Mn^{2+}(^6A_1) \xrightarrow{ET1} Mn^{2+}(^4T_1) \xrightarrow{h\nu} Mn^{3+} + e_{CB} \quad (\text{or } Mn^{2+} + e_{CB} + h_{local}) \tag{2}$$

In their study, the 440 nm beam was used for the excitation of the exciton and the 676 nm beam was used to excite the $^4T_1$ state to the conduction band. However, since the absorption cross section of the $^4T_1$ state was several orders of magnitude smaller than that of the exciton, the 676 nm beam was several orders of magnitude more intense than the 440 nm beam to excite the $^4T_1$ state to the conduction band resonantly. The decrease of Mn luminescence intensity upon excitation from the $^4T_1$ state to the conduction band is considered to be due to the relatively fast nonradiative relaxation pathway compared to the relaxation of the electron through the manifold of ligand field states of Mn^{2+} ion. The nonradiative decay of the electrons ionized from Mn^{2+} ions to the conduction band was also reported in Mn-doped ZnO nanocrystals, where the direct charge transfer excitation from $^6A_1$ state to conduction band can occur with sub-bandgap excitation due to the midgap location of the $^6A_1$ state.[24] (eq 3) However, such direct charge

dx.doi.org/10.1021/jp2016598 |J. Phys. Chem. C 2011, 115, 11407–11412

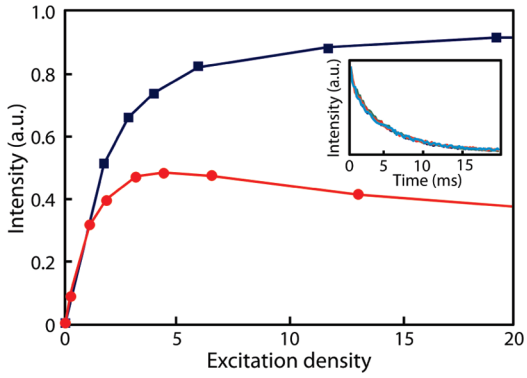

Figure 4. Excitation density-dependent luminescence of undoped (blue) and Mn-doped (red) CdS/ZnS core/shell nanocrystals. The lines are a visual guide. The inset compares the Mn luminescence decay curves at the excitation density of 2.5, 5, and 15 photons/particle.

transfer excitation does not occur in Mn-doped CdS/ZnS nanocrystals.

$$Mn^{2+}({}^6A_1) \xrightarrow{h\nu} Mn^{3+} + e_{CB} \quad (\text{or } Mn^{2+} + e_{CB} + h_{local}) \quad (3)$$

In our study, we observed the decrease of Mn luminescence intensity in Mn-doped CdS/ZnS nanocrystals as the excitation density increased under pulsed excitation conditions, which can only be explained by the excitation of hot electrons via two consecutive energy transfers. We used pulsed excitation at 395 nm (60 fs pulse width) in the fluence range of 0−4.6 mJ/cm^2 per pulse. Under this condition, the probability of resonant excitation of the $^4T_1$ state to the conduction band is negligible, since the absorption cross section of the $^4T_1$ state at 395 nm is estimated to be 3−4 orders of magnitude smaller than that of the exciton ($\sigma_{ex} = 2.2 \times 10^{-15}$ cm^2) in our Mn-doped nanocrystals.[19,25] Therefore, the process described in eq 2 is highly unlikely under our experimental conditions. In addition, the excitation pulse width (60 fs) much shorter than the exciton−Mn energy transfer time (~10 ps)[26] and the slow rate (50 Hz) of the excitation further preclude the possibility of the excitation of the $^4T_1$ state to the conduction band following ET1. Furthermore, the lattice heating from the photoexcitation is sufficiently small and short-lived, not affecting the luminescence lifetime and quantum yield of the $^4T_1$ state as will be discussed further in detail below. This indicates that the decrease of Mn luminescence reflects the actual depletion of the emitting $^4T_1$ state population.

Figure 4 compares the excitation density-dependent luminescence intensities of Mn-doped (red) and undoped (blue) CdS/ZnS nanocrystals in the excitation density of 0−20 photons/particle. The two curves are plotted with the initial slopes in the linear regime at low excitation densities matched in order to show the difference at higher excitation densities more clearly. The average excitation density, $\langle n_{ex} \rangle$, was estimated from $\langle n_{ex} \rangle = f \cdot \sigma$, where f is the excitation fluence and σ is the absorption cross section of the nanocrystal assuming that σ is not sensitive to the excitation intensity. Although this assumption is not strictly true, the measurement of the transmittance of the excitation beam through the sample indicated that σ is only very weakly dependent on the excitation fluences of our study.

In Figure 4, the intensity of Mn luminescence in Mn-doped nanocrystals increases initially at low excitation density regime (0−3 photons/particle) but decreases as the excitation density increases further. No noticeable change of the luminescence spectrum was observed within the entire range of the excitation density. The inset in Figure 4 shows the decay of Mn luminescence intensity in time at several different excitation densities: 2.5, 5, and 15 photons/particle. It shows nearly identical decay at all the excitation densities with the decay time of ~5 ms, indicating that the relaxation channels of the $^4T_1$ state do not vary within the range of the excitation densities of this study. The initial transient lattice temperature rise from the photoexcitation (ΔT_{max} ~25 K for 20 photon/particle)[27] does not seem to influence the lifetime of the $^4T_1$ state, since the small nanocrystals suspended in liquid solvent cool very rapidly (e.g., ~100 ps for <10 nm diameter).[28] On the other hand, the exciton luminescence intensity of undoped nanocrystal sample exhibits a quite different behavior. The exciton luminescence intensity increases initially and saturates at higher excitation densities, consistent with the previous observation made in CdSe nanocrystals by Fisher et al.[29] In undoped nanocrystals, multiexciton state rapidly falls back to one-exciton state. Therefore, the majority of the exciton luminescence intensity is contributed by the one-exciton state with a minor contribution from the multiexciton state resulting in the saturation of exciton luminescence intensity as observed.

As mentioned above, the direct resonant excitation from the $^4T_1$ state to the conduction band following ET1 is highly unlikely under our experimental conditions. Furthermore, while Auger-type deexcitation of the $^4T_1$ state by an extra electron in the conduction band may be a possible additional relaxation channel of the $^4T_1$ state reducing Mn luminescence lifetime, such a process does not seem to occur either in our study.[30] On the other hand, the depletion of the $^4T_1$ state can occur via two consecutive exciton−Mn energy transfers from multiple numbers of excitons if both ET1 and ET2 are sufficiently fast compared to the exciton relaxation and decay of the intermediate acceptor state ($^4T_1$). In our previous study, the time scale of ET1 between a pair of exciton and Mn^{2+} ion in Mn-doped CdS/ZnS nanocrystal was determined to be tens of picoseconds for a single exciton−Mn pair, and the energy transfer became faster with increasing Mn doping density.[26] Moreover, the energy transfer was sufficiently fast even when Auger recombination was present at high exciton densities in the nanocrystals.[26] Considering that ET1 and ET2 are essentially the same type of energy transfer with a difference in the accepting Mn ligand field transitions, it is reasonable to expect that the rates of both energy transfer processes are of a similar order of magnitude. In such case, the two consecutive energy transfers to one acceptor can occur effectively competing with two individual energy transfer processes to two acceptors before the relaxation of all the excitons when multiple numbers of excitons are excited in the nanocrystals.

Unlike in usual two-photon processes quadratic to the excitation intensity, the two consecutive exciton−Mn energy transfer processes in Mn-doped nanocrystals will not exhibit such quadratic behavior since the density of excitons varies with time during the energy transfer process. Therefore, hot electron generation via two consecutive energy transfers cannot be confirmed by checking the presence of the quadratic excitation intensity dependence. However, further corroborating evidence for the occurrence of two consecutive exciton−Mn energy transfers can be obtained from the comparison of Mn luminescence intensities under one- and two-pulse excitation conditions, as shown in Figure 5. For the two-pulse excitation, the second pulse with the equal intensity as the first pulse is applied 200 ps after the first pulse, which is much longer than the time scale of ET1. At low excitation densities (e.g., <2 photons/particle) the

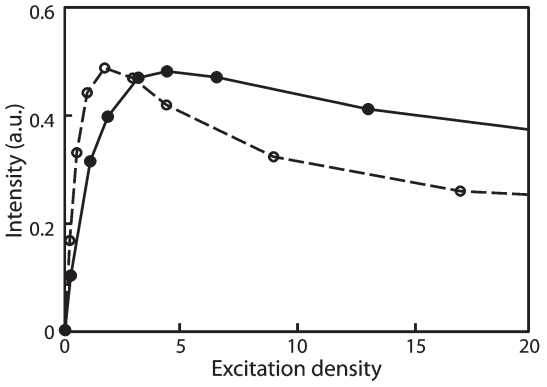

Figure 5. Excitation density-dependent luminescence intensity of Mn-doped nanocrystals under one-pulse (solid) and two-pulse (dashed) excitation. For the two-pulse excitation, the pulses are separated by 200 ps. The lines are a visual guide.

effect of the second pulse is increasing Mn luminescence intensity. On the other hand, the second pulse results in the decrease of Mn luminescence intensity at the excitation densities higher than ~3 photons/particle.

The opposite effect of the second pulse on Mn luminescence intensity in different excitation density regimes can be understood from the different relative magnitudes of $k_{ET1}[^6A_1]$ and $k_{ET2}[^4T_1]$. Here, k_{ET1} and k_{ET2} are the rate constants of ET1 and ET2 processes for a single donor−acceptor pair. $[^6A_1]$ and $[^4T_1]$ are the populations of the two Mn^{2+} ligand field states at the time of the excitation by the second pulse. Therefore, $k_{ET1}[^6A_1]$ and $k_{ET2}[^4T_1]$ represent, respectively, the rate of population and depletion of the $^4T_1$ state via energy transfer from each exciton excited by the second pulse. At low excitation densities, $k_{ET1}[^6A_1]$ will be larger than $k_{ET2}[^4T_1]$ since the majority of Mn^{2+} ions are at the ground $^6A_1$ state. Therefore, the net effect of the second pulse is increasing the population of the $^4T_1$ state via ET1, resulting in the further increase of Mn luminescence intensity. As the excitation density from the first pulse increases, $k_{ET1}[^6A_1]$ decreases while $k_{ET2}[^4T_1]$ increases. Therefore, ET2 will become the increasingly more dominating process in the excitation by the second pulse, resulting in the depletion of the $^4T_1$ state and the decrease of Mn luminescence intensity as observed in this study. However, if ET2 does not occur or is not sufficiently fast compared to the exciton relaxation, the second pulse should result in only the increase and saturation of Mn luminescence intensity as the excitation density increases.

The fact that the second pulse has no net effect on Mn luminescence at the excitation density of ~3 photons/particle in the nanocrystals with Mn doping density of 3.6 ions/particle and Mn luminescence quantum yield of ~40% suggests that the rates of ET1 and ET2 are of similar order of magnitude. In principle, Mn luminescence intensity vs initial excitation density can be simulated with an appropriate kinetic model to extract the rate of ET2 if the rates of all other dynamic processes in play are known. However, the complexity of the kinetics that includes various competing linear and nonlinear processes and uncertainties of some rate parameters in addition to Poisson distribution of dopant ions requiring statistical averaging of k_{ET1} and k_{ET2} make it difficult to extract an accurate rate of ET2 at this point.

Since both ET1 and ET2 are many orders of magnitude faster than the decay of the $^4T_1$ state (τ = 5 ms), two consecutive exciton−Mn energy transfers can generate hot electrons even

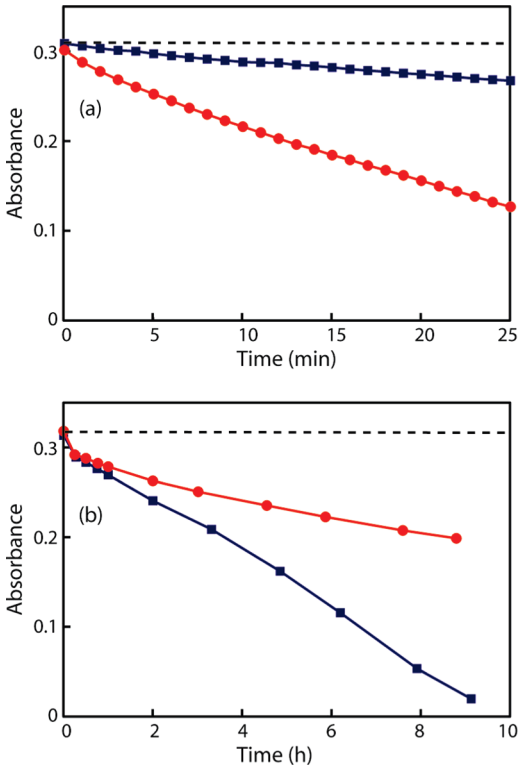

Figure 6. Photocatalytic reduction of MB in undoped (blue squares) and Mn-doped (red circles) solution under (a) 760 and (b) 1.2 mW/cm^2 405 nm cw excitation. The solid lines are a visual guide. The dashed lines are the initial absorbance of MB.

with cw excitation as long as the excitation rate is sufficiently fast to allow ET2 before the decay of the $^4T_1$ state. In this regard, the long $^4T_1$ state lifetime is particularly beneficial for having consecutive energy transfer from cw excitation. Hot electrons generated in Mn-doped nanocrystals in this way can potentially be useful for photocatalytic reduction reaction taking advantage of the lower energy barrier and larger donor−acceptor electronic coupling of the electrons of higher energy for the electron transfer.[31] In order to test whether photocatalysis by Mn-doped nanocrystals can benefit from consecutive exciton−Mn energy transfer under cw excitation, the photocatalytic reduction efficiencies of undoped and Mn-doped nanocrystals were compared at two different excitation conditions: (a) fast excitation rate allowing consecutive exciton−Mn energy transfer and (b) slow excitation rate with no consecutive exciton−Mn energy transfer. The comparison of the reduction efficiencies was made using the photocatalytic reduction of methylene blue (MB). Photocatalytic reduction of MB in the absence of the dissolved oxygen in solution is known to lead to the disappearance of the color in the visible via the formation of colorless leucomethylene blue.[32] To prevent the degradation of MB via oxidative mineralization by the dissolved oxygen that also results in the loss of color, the measurement was made under O_2-free environment using the deoxygenated dichloromethane as the solvent.[33] Due to the simplicity of the colorimetric measurement, MB has been used to assess the efficiency in heterogeneous photocatalytic reduction in many studies.[34−36]

Figure 6a and b compare the decay kinetics of the absorption of MB at 656 nm by undoped (blue) and Mn-doped (red) nanocrystals under 405 nm cw excitation at two different

dx.doi.org/10.1021/jp2016598 |J. Phys. Chem. C 2011, 115, 11407–11412

excitation conditions mentioned above. For the data in Figure 6a, the average excitation intensity within the full-width at half-maximum (fwhm) from a 405 nm diode laser was 760 mW/cm^2 corresponding to the average excitation rate of 12 excitations/$^4T_1$ lifetime for each particle. At this excitation rate, two consecutive energy transfers can occur in Mn-doped nanocrystals. For the data in Figure 6b, a 405 nm light emitting diode was used for the excitation at the intensity of 1.2 mW/cm^2 corresponding to the average excitation rate of 0.02 excitations/$^4T_1$ lifetime. At this slow excitation rate, only the isolated single energy transfer events can occur in Mn-doped nanocrystals.

In Figure 6a, the kinetics is ~4 times faster in Mn-doped nanocrystals than in undoped nanocrystals. On the other hand, undoped nanocrystals exhibit faster kinetics than Mn-doped nanocrystals in Figure 6b. The opposite trend of the photocatalytic efficiencies of Mn-doped and undoped nanocrystals under the two different excitation conditions may be explained in the following way. At the slower excitation rate, the role of exciton−Mn energy transfer is simply decreasing the exciton density within the nanocrystals resulting in the lower photocatalytic reduction efficiency of Mn-doped nanocrystals compared to the undoped ones. At the higher excitation rate, two consecutive exciton−Mn energy transfers can generate hot electrons and localized holes. Hot electrons with a large excess energy can exhibit higher reduction efficiency than electrons from near-band edge excitons in undoped nanocrystals, more than compensating the smaller number of electrons generated. The above result indicates that consecutive energy transfer in Mn-doped nanocrystals has a beneficial effect in photocatalysis, while further studies on the reaction involving both electron and holes are needed to reveal its full potential.

4. CONCLUSION

In summary, we investigated the occurrence of consecutive exciton−Mn energy transfer in Mn-doped semiconductor nanocrystals that can generate hot electrons with a large excess energy in the conduction band. Due to the fast exciton−Mn energy transfer and long lifetime of the intermediate acceptor state, two consecutive exciton−Mn energy transfers can occur efficiently even with relatively weak cw excitation. Under the excitation condition that supports consecutive exciton−Mn energy transfer responsible for hot electron generation, Mn-doped nanocrystals exhibit higher photocatalytic reduction efficiency than undoped nanocrystals.

AUTHOR INFORMATION

Corresponding Author

*E-mail: dhson@mail.chem.tamu.edu.

ACKNOWLEDGMENT

This work was supported partially by the Welch Foundation (Grant No. A-1639). K.L. was supported by NSF-REU program (CHE-0755207). We thank Microscopy and Imaging Center and Elemental Analysis Laboratory of Texas A&M University for TEM and ICP-MS measurements.

REFERENCES

(1) Zhu, X. Y. *Annu. Rev. Phys. Chem.* **1994**, *45*, 113.
(2) Park, J. Y.; Somorjai, G. A. *J. Vac. Sci. Technol., B* **2006**, *24*, 1967.
(3) Brus, L. *Acc. Chem. Res.* **2008**, *41*, 1742.
(4) Gadzuk, J. W. *Phys. Rev. Lett.* **1996**, *76*, 4234.
(5) Gaillard, F.; Sung, Y.-E.; Bard, A. J. *J. Phys. Chem. B* **1999**, *103*, 667.
(6) Bonn, M.; Funk, S.; Hess, C.; Denzler, D. N.; Stampfl, C.; Scheffler, M.; Wolf, M.; Ertl, G. *Science* **1999**, *285*, 1042.
(7) Nozik, A. J. *Annu. Rev. Phys. Chem.* **2001**, *52*, 193.
(8) Ross, R. T.; Nozik, A. J. *J. Appl. Phys.* **1982**, *53*, 3813.
(9) Anderson, N. A.; Lian, T. *Annu. Rev. Phys. Chem.* **2005**, *56*, 491.
(10) Tisdale, W. A.; Williams, K. J.; Timp, B. A.; Norris, D. J.; Aydil, E. S.; Zhu, X. Y. *Science* **2010**, *328*, 1543.
(11) Pandey, A.; Guyot-Sionnest, P. *J. Phys. Chem. Lett.* **2010**, *1*, 45.
(12) Huang, J.; Huang, Z.; Yang, Y.; Zhu, H.; Lian, T. *J. Am. Chem. Soc.* **2010**, *132*, 4858.
(13) Schmidt, M. E.; Blanton, S. A.; Hines, M. A.; Guyot-Sionnest, P. *Phys. Rev. B* **1996**, *53*, 12629.
(14) Son, D. H.; Wittenberg, J. S.; Alivisatos, A. P. *Phys. Rev. Lett.* **2004**, *92*, 127406.
(15) Chon, J. W. M.; Gu, M.; Bullen, C.; Mulvaney, P. *Appl. Phys. Lett.* **2004**, *84*, 4472.
(16) Bol, A. A.; Meijerink, A. *Phys. Rev. B* **1998**, *58*, R15997.
(17) Beaulac, R.; Archer, P. I.; Ochsenbein, S. T.; Gamelin, D. R. *Adv. Funct. Mater.* **2008**, *18*, 3873.
(18) Irvine, S.; Staudt, T.; Rittweger, E.; Engelhardt, J.; Hell, S. *Angew. Chem., Int. Ed.* **2008**, *47*, 2685.
(19) Dreyhsig, J.; Allen, J. W. *J. Phys.: Condens. Matter* **1989**, *1*, 1087.
(20) Yu, W. W.; Peng, X. *Angew. Chem., Int. Ed.* **2002**, *41*, 2368.
(21) Yang, Y.; Chen, O.; Angerhofer, A.; Cao, Y. C. *J. Am. Chem. Soc.* **2008**, *130*, 15649.
(22) Taniguchi, M.; Fujimori, M.; Fujisawa, M.; Mori, T.; Souma, I.; Oka, Y. *Solid State Commun.* **1987**, *62*, 431.
(23) Nazir, S.; Ikram, N.; Tanveer, M.; Shaukat, A.; Saeed, Y.; Reshak, A. H. *J. Phys. Chem. A* **2009**, *113*, 6022.
(24) Norberg, N. S.; Kittilstved, K. R.; Amonette, J. E.; Kukkadapu, R. K.; Schwartz, D. A.; Gamelin, D. R. *J. Am. Chem. Soc.* **2004**, *126*, 9387.
(25) Kushida, T.; Tanaka, Y.; Oka, Y. *Solid State Commun.* **1974**, *14*, 617.
(26) Chen, H.-Y.; Chen, T.-Y.; Son, D. H. *J. Phys. Chem. C* **2010**, *114*, 4418.
(27) The maximum change in temperature in nanocrystal lattice (ΔT_{max}) by the absorption of light was obtained from $E = mC\Delta T_{max}$, where E, m, and C are the total energy of photons absorbed by each nanocrystal (1.01×10^{-17} J for 20 photon absorption), mass (8.9×10^{-19} g), and specific heat (0.47 J/gK) of nanocrystal, respectively. Actual lattice temperature will be lower than that from this estimate.
(28) Chen, T.-Y.; Hsia, C.-H.; Son, D. H. *J. Phys. Chem. C* **2008**, *112*, 10125.
(29) Fisher, B.; Caruge, J.-M.; Chan, Y.-T.; Halpert, J.; Bawendi, M. G. *Chem. Phys.* **2005**, *318*, 71.
(30) White, M. A.; Weaver, A. L.; Beaulac, R. m.; Gamelin, D. R. *ACS Nano* **2011**, doi: 10.1021/nn200889q.
(31) Asbury, J. B.; Hao, E.; Wang, Y.; Ghosh, H. N.; Lian, T. *J. Phys. Chem. B* **2001**, *105*, 4545.
(32) Sheps, L.; Crowther, A. C.; Elles, C. G.; Crim, F. F. *J. Phys. Chem. A* **2005**, *109*, 4296.
(33) Mills, A.; Wang, J. *J. Photochem. Photobiol., A* **1999**, *127*, 123.
(34) Costi, R.; Saunders, A. E.; Elmalem, E.; Salant, A.; Banin, U. *Nano Lett.* **2008**, *8*, 637.
(35) Huang, Y.; Sun, F.; Wang, H.; He, Y.; Li, L.; Huang, Z.; Wu, Q.; Yu, J. C. *J. Mater. Chem.* **2009**, *19*, 6901.
(36) Fang, F.; Chen, L.; Chen, Y.-B.; Wu, L.-M. *J. Phys. Chem. C* **2010**, *114*, 2393.